Available online at www.sciencedirect.com
ScienceDirect
International Journal of Heat and Fluid Flow 28 (2007) 15–27
International Journal of HEAT AND FLUID FLOW
www.elsevier.com/locate/ijhff

Effects of viscous dissipation and temperature dependent viscosity in thermally and simultaneously developing laminar flows in microchannels

S. Del Giudice, C. Nonino *, S. Savino

Dipartimento di Energetica e Macchine, Università degli Studi di Udine, Via delle Scienze 208, 33100 Udine, Italy

Received 11 May 2006; accepted 20 May 2006
Available online 21 August 2006

Abstract

The effects of viscous dissipation and temperature dependent viscosity in both thermally and simultaneously developing laminar flows of liquids in straight microchannels of arbitrary, but constant, cross-sections are studied. In order to allow a parametric investigation, viscosity is assumed to vary linearly with temperature, while the other fluid properties are held constant. Different cross-sectional geometries are considered, chosen among those usually adopted for microchannels. Reference is made to uniform wall temperature boundary conditions. A finite element procedure is employed for the solution of the parabolized momentum and energy equations. Computed axial distributions of the local Nusselt number and of the apparent Fanning friction factor for ducts of the considered cross-sections are presented with reference to both heating and cooling conditions. Numerical results confirm that, in the laminar forced convection in straight microchannels, both temperature dependence of viscosity and viscous dissipation effects cannot be neglected in a wide range of operative conditions.

Keywords: Laminar forced convection; Straight ducts; Thermally developing flows; Simultaneously developing flows; Temperature dependent viscosity; Viscous heating

1. Introduction

In laminar flows in microchannels, fluid velocity and temperature fields do not very often develop simultaneously since fluid heating or cooling may begin at an axial position which does not coincide with the microchannel inlet. In general, heating or cooling will start at an axial location where the flow, from a hydrodynamic point of view, is only partially developed, with a virtually infinite number of possible combinations. However it can be confidently assumed that most situations of practical interest will fall between the two limiting cases corresponding to thermally developing flow (when heating or cooling begins at a position along the microchannel where hydrodynamically fully developed conditions have already been reached) and simultaneously developing flow (when heating or cooling begins at the microchannel inlet). In all these cases, entrance effects on forced convection heat transfer cannot be neglected if, as it happens very often in laminar flows, the total length of the heated/cooled part of the microchannel is comparable with that of the entrance region. Moreover, temperature dependence of fluid properties can also play an important role in the development of the thermal field, modifying both heat fluxes and velocity distributions. If, as it is assumed in this paper, the fluid is a liquid, viscosity is the property which exhibits the most relevant variations with respect to temperature. Therefore, the main effects of temperature dependent fluid properties can be retained even if only viscosity is allowed to vary with temperature, while the other properties are assumed constant.

* Corresponding author. Tel.: +39 0432 558019; fax: +39 0432 558027.
E-mail address: carlo.nonino@uniud.it (C. Nonino).

0142-727X/$ - see front matter © 2006 Elsevier Inc. All rights reserved.
doi:10.1016/j.ijheatfluidflow.2006.05.007

Nomenclature

A	area of the cross-section (m^2)
a	height of the cross-section (m)
Br	Brinkman number, $Br = \mu\bar{u}^2/[k(t_e - t_w)]$
b	base of the cross-section (m)
c	specific heat (J/kg K)
D_h	hydraulic diameter (m)
f	Fanning friction factor (–)
h	convection coefficient (W/m^2 K)
k	thermal conductivity (W/m K)
Nu	Nusselt number, $Nu = hD_h/k$
P	perimeter of the cross-section (m)
P_t	heated/cooled perimeter (m)
Pe	Péclet number, $Pe = RePr$
Pr	Prandtl number, $Pr = \mu c/k$
p	deviation from the hydrostatic pressure (Pa)
q'	heat transfer rate per unit length (W/m)
q''	heat flux (W/m^2)
Re	Reynolds number, $Re = \rho\bar{u}D_h/\mu$
r	radial coordinate (m)
T	dimensionless temperature, $T = (t - t_w)/(t_e - t_w)$
T'	dimensionless temperature, $T' = (t - t_w)/(t_b - t_w)$
t	temperature (°C)
U	dimensionless axial velocity, $U = u/\bar{u}$
u, v, w	velocity components (m/s)
X^+	dimensionless axial coordinate, $X^+ = x/D_h\, Re_m$
X^*	dimensionless axial coordinate, $X^* = x/D_h Pe$
x	axial coordinate (m)
y, z	transverse Cartesian coordinates (m)

Greek symbols

α	parameter in Eq. (14) (kg/m s K)
β	parameter in Eq. (15) (K^{-1})
γ	aspect ratio of the cross-section, $\gamma = a/b$
μ	dynamic viscosity (kg/m s)
ρ	density (kg/m^3)

Subscripts and superscripts

A	in axisymmetric coordinates
a	apparent
b	bulk
C	in Cartesian coordinates
c	constant property
e	entrance
m	reference, evaluated at t_m
o	outer
w	wall
−	average value
∞	asymptotic value

It must be pointed out that, in such a case, dependence of viscosity on temperature influences the thermal field by modifying the velocity distribution in the heated/cooled part of the channel. Finally, viscous dissipation effects cannot often be neglected in ducts with very small hydraulic diameters, like microchannels, even for ordinary liquids, characterised by moderate values of viscosity. It is worth noting that, with temperature dependent viscosity, viscous dissipation modifies both temperature and velocity distributions along the whole microchannel, in much the same way as wall heat transfer does. Even if these effects have already been considered in the past, to the authors' knowledge no systematic studies are reported in the literature taking into account the combination of entrance, temperature dependent viscosity and viscous dissipation effects.

In the past decades, many authors have investigated, either analytically or numerically, both thermally developing flows and simultaneously developing flows in straight ducts of constant cross-section. Comprehensive reviews of these theoretical studies, referring to ducts of different cross-sectional geometries, can be found in Shah and London (1978) and Shah and Bhatti (1987). However, since a basic assumption made in almost all such studies is that fluid properties are constant, the corresponding solutions are adequate only for problems involving small temperature differences. In fact, experimental results for problems involving large temperature differences substantially deviate from constant property solutions (Shah and London, 1978; Kakaç, 1987).

As anticipated above, for most liquids, the density, specific heat and thermal conductivity are nearly independent of temperature, while viscosity markedly decreases with increasing temperature, in much the same manner as the Prandtl number does (Kakaç, 1987). Thus, the assumption of constant properties, with the exception of viscosity, which is still allowed to vary with temperature, is adequate for most liquid flows, no matter how large the temperature differences are. Because of the relative complexity of temperature dependent property problems, only a limited number of such solutions for laminar forced convection in both thermally and simultaneously developing flows in ducts have appeared in the literature (Shah and London, 1978). However, most of these studies are based on the assumption of a viscosity dependence on temperature given by specific relations of empirical nature (Kakaç, 1987; Nouar, 1999; Nóbrega et al., 2004), leading to results which cannot be considered general and applicable to other liquids or for different temperature ranges. Similar considerations can be made with respect to studies concerning thermally or simultaneously developing flows in microchannels (Toh et al., 2002; Xu et al., 2003; Koo and Kleinstreuer, 2004a; Koo and Kleinstreuer, 2004b). To allow a generalization of

the results, Berardi and Cuccurullo (2000) and Sahin (1999) assumed a linear viscosity–temperature relation. It is worth noting that a linear temperature dependence of viscosity can always be obtained by approximating the appropriate relation by a Taylor series expansion truncated at the first order term (Berardi and Cuccurullo, 2000).

In laminar flows in macrochannels, except for the case of very viscous fluids at relatively high velocity, viscous dissipation effects can be ignored (Shah and London, 1978; Morini, 2005a; Shen et al., 2004; Cuccurullo and Berardi, 2000), since their contribution to the energy balance is negligible (Shen et al., 2004). Therefore, viscous dissipation effects in laminar forced convection are usually studied only with reference to very high Prandtl number fluids, for which hydrodynamically fully developed conditions can be reasonably assumed at the entrance. For this reason, almost all existing studies concern fully developed forced convection (Barletta, 1997) or thermally developing and hydrodynamically fully developed flows (Lin et al., 1983; Basu and Roy, 1985; Zanchini, 1997). Since, in all these studies, the assumption of a constant property fluid is made, the velocity profile is assumed to remain the same along the whole channel length. Instead, viscous dissipation effects cannot be ignored in microchannel flows of ordinary fluids, having Prandtl numbers of the order of few units, due to the very small values of the hydraulic diameter (Morini, 2005a; Morini, 2005b; Shen et al., 2004; Koo and Kleinstreuer, 2003; Herwig and Hausner, 2003; Tso and Mahulikar, 1998). For such fluids, hydrodynamic and thermal entrance lengths are comparable, so that it is reasonable to assume either fully developed or uniform velocity profiles at the entrance of the heated/cooled part of the microchannel, resulting in thermally developing and hydrodynamically fully developed flow or in simultaneously developing flow, respectively. Therefore, existing literature on viscous dissipation effects in microchannels does not only consider fully developed forced convection (Morini, 2005a; Morini, 2005b; Shen et al., 2004) and thermally developing and hydrodynamically fully developed flow (Koo and Kleinstreuer, 2004a; Koo and Kleinstreuer, 2004b; Tunc and Bayazitoglu, 2001), but also simultaneously developing flow (Toh et al., 2002; Xu et al., 2003). It must be pointed out that if, as in most of these studies, a temperature dependent viscosity is assumed, the velocity distribution varies in the thermal entrance region even when a fully developed velocity profile is assumed at the axial position where fluid heating/cooling begins. However, this fully developed velocity profile depends both on viscous dissipation, which is responsible for the non-uniform fully developed temperature profile, and on temperature dependence of viscosity, which, in turn, distorts the velocity profile with respect to the constant property case.

In this paper, we present the results of a parametric study on both thermally and simultaneously developing laminar flows of liquids in straight microchannels of arbitrary, but constant, cross-sections. The effects of temperature dependent viscosity and viscous dissipation on heat transfer and pressure drop are investigated, while the other liquid properties are considered constant. A finite element procedure (Nonino et al., 1988), based on a projection algorithm (Patankar and Spalding, 1972), is employed for the step-by-step solution of the parabolized momentum and energy equations in a two-dimensional domain corresponding to the cross-section of the duct (Patankar and Spalding, 1972; Hirsh, 1988). Due to the high value of the ratio between the total length and the hydraulic diameter in microchannels, such an approach is very advantageous with respect to the one based on the steady-state solution of the elliptic form of the governing equations in a three-dimensional domain corresponding to the whole microchannel. The procedure has already been used, disregarding viscous dissipation effects, in the simulation of simultaneously developing flows of liquids with temperature dependent viscosity in straight macro- and microchannels (Nonino et al., 2005a; Nonino et al., 2005b). Here, the procedure is also validated for non-negligible viscous dissipation effects with reference to thermal entrance flow of a constant property fluid in circular ducts (Basu and Roy, 1985). New results concern different cross-sectional geometries, chosen among those usually adopted for microchannels (Morini, 2005a; Morini, 2005b), namely circular, rectangular with aspect ratio $\gamma = 0$ (parallel plates) and trapezoidal with $\gamma = 0.414$. In all the cases studied here, reference is made to uniform wall temperature boundary conditions and, in order to allow a parametric investigation, viscosity is assumed to vary linearly with temperature in the range considered.

2. Mathematical model

When the effects of axial diffusion can be neglected and there is no recirculation in the longitudinal direction, steady-state flow and heat transfer in straight microchannels of constant cross-section are governed by the continuity and the parabolized Navier–Stokes and energy equations. Since the inverse of the Reynolds number is representative of the relative importance of diffusive and advective components of the axial momentum flow rate, while the inverse of the Péclet number is representative of the relative importance of conductive and advective components of the axial heat flow rate, the parabolic approximation of the Navier–Stokes and energy equations can be considered adequate, except in the immediate neighborhood of the inlet, for values of the Reynolds and Péclet numbers larger than 50 (Shah and London, 1978; Javeri, 1977). With reference to incompressible fluids with temperature dependent thermophysical properties, in the hypotheses of negligible body forces and significant effects due to viscous dissipation, these equations can be written in the following forms, valid for three-dimensional and axisymmetric geometries, respectively.

For three-dimensional geometries, the governing equations are

$$\frac{\partial}{\partial x}(\rho u)+\frac{\partial}{\partial y}(\rho v)+\frac{\partial}{\partial z}(\rho w)=0 \tag{1}$$

$$\rho u\frac{\partial u}{\partial x}=\frac{\partial}{\partial y}\left(\mu\frac{\partial u}{\partial y}\right)+\frac{\partial}{\partial z}\left(\mu\frac{\partial u}{\partial z}\right)-\rho v\frac{\partial u}{\partial y}-\rho w\frac{\partial u}{\partial z}-\frac{\mathrm{d}\bar{p}}{\mathrm{d}x} \tag{2}$$

$$\rho u\frac{\partial v}{\partial x}=\frac{\partial}{\partial y}\left[2\mu\frac{\partial v}{\partial y}-\frac{2}{3}\left(\mu\frac{\partial v}{\partial y}+\mu\frac{\partial w}{\partial z}\right)\right]+\frac{\partial}{\partial z}\left(\mu\frac{\partial w}{\partial y}+\mu\frac{\partial v}{\partial z}\right)-\rho v\frac{\partial v}{\partial y}-\rho w\frac{\partial v}{\partial z}-\frac{\partial p}{\partial y} \tag{3}$$

$$\rho u\frac{\partial w}{\partial x}=\frac{\partial}{\partial z}\left[2\mu\frac{\partial w}{\partial z}-\frac{2}{3}\left(\mu\frac{\partial v}{\partial y}+\mu\frac{\partial w}{\partial z}\right)\right]+\frac{\partial}{\partial y}\left(\mu\frac{\partial w}{\partial y}+\mu\frac{\partial v}{\partial z}\right)-\rho v\frac{\partial w}{\partial y}-\rho w\frac{\partial w}{\partial z}-\frac{\partial p}{\partial z} \tag{4}$$

$$\rho cu\frac{\partial t}{\partial x}=\frac{\partial}{\partial y}\left(k\frac{\partial t}{\partial y}\right)+\frac{\partial}{\partial z}\left(k\frac{\partial t}{\partial z}\right)-\rho cv\frac{\partial t}{\partial y}-\rho cw\frac{\partial t}{\partial z}+\mu(\Phi_{\mathrm{v}})_{\mathrm{C}} \tag{5}$$

where

$$(\Phi_{\mathrm{v}})_{\mathrm{C}}=2\left[\left(\frac{\partial v}{\partial y}\right)^2+\left(\frac{\partial w}{\partial z}\right)^2\right]+\left(\frac{\partial w}{\partial y}+\frac{\partial v}{\partial z}\right)^2+\left(\frac{\partial u}{\partial y}\right)^2+\left(\frac{\partial u}{\partial z}\right)^2-\frac{2}{3}\left(\frac{\partial v}{\partial y}+\frac{\partial w}{\partial z}\right)^2 \tag{6}$$

while for axisymmetric geometries, they become

$$\frac{\partial}{\partial x}(\rho u)+\frac{1}{r}\frac{\partial}{\partial r}(\rho rv)=0 \tag{7}$$

$$\rho u\frac{\partial u}{\partial x}=\frac{1}{r}\frac{\partial}{\partial r}\left(\mu r\frac{\partial u}{\partial r}\right)-\rho v\frac{\partial u}{\partial r}-\frac{\mathrm{d}\bar{p}}{\mathrm{d}x} \tag{8}$$

$$\rho u\frac{\partial v}{\partial x}=\frac{2}{r}\left[\frac{\partial}{\partial r}\left(\mu r\frac{\partial v}{\partial r}\right)-\mu\frac{v}{r}\right]-\frac{2}{3r}\left\{\frac{\partial}{\partial r}\left[\mu\frac{\partial}{\partial r}(rv)\right]+\frac{\mu}{r}\frac{\partial}{\partial r}(rv)\right\}-\rho v\frac{\partial v}{\partial r}-\frac{\partial p}{\partial r} \tag{9}$$

$$\rho cu\frac{\partial t}{\partial x}=\frac{1}{r}\frac{\partial}{\partial r}\left(kr\frac{\partial t}{\partial r}\right)-\rho cv\frac{\partial t}{\partial r}+\mu(\Phi_{\mathrm{v}})_{\mathrm{A}} \tag{10}$$

where

$$(\Phi_{\mathrm{v}})_{\mathrm{A}}=\left(\frac{\partial u}{\partial r}\right)^2+2\left[\left(\frac{\partial v}{\partial r}\right)^2+\left(\frac{v}{r}\right)^2\right]-\frac{2}{3}\left(\frac{\partial v}{\partial r}+\frac{v}{r}\right)^2 \tag{11}$$

According to the assumption of parabolic flow, all the derivatives in the axial direction are neglected in the diffusive terms of the above equations (Hirsh, 1988). In the set of equations valid for three-dimensional geometries, x, y and z are the axial and the transverse coordinates, respectively, while u, v and w represent the axial and the transverse components of velocity. In the axisymmetric equations, symbols r and v denote the radial coordinate and the radial component of velocity. Finally, t is the temperature, p is the deviation from the hydrostatic pressure, $\bar{p}$ is its average value over the cross-section, while ρ, μ, c and k represent density, dynamic viscosity, specific heat and thermal conductivity of the fluid, respectively.

The solution domain can be bounded by rigid walls or symmetry axes. The usual no-slip conditions are applied on rigid boundaries, that is, $u=v=w=0$ for three-dimensional geometries and $u=v=0$ in the axisymmetric case, while the temperature is prescribed ($t=t_{\mathrm{w}}$). Symmetry conditions, instead, are $\partial u/\partial y=\partial w/\partial y=0$, $v=0$ and $\partial t/\partial y=0$ on boundaries perpendicular to the y axis, $\partial u/\partial z=\partial v/\partial z=0$, $w=0$ and $\partial t/\partial z=0$ on boundaries perpendicular to the z axis for three-dimensional geometries, and $\partial u/\partial r=0$, $v=0$ and $\partial t/\partial r=0$ at the symmetry axis in axisymmetric problems.

The model equations are solved using a finite element procedure which represents an extended version of the one previously developed for the analysis of the forced convection of constant property fluids in the entrance region of straight ducts (Nonino et al., 1988). The added new features mainly consist in the possibility of taking into account the effects of temperature dependent properties and of viscous dissipation. The adopted procedure is based on a segregated approach which implies the sequential solution of the momentum and energy equations on a two-dimensional domain in the case of three-dimensional geometries and on a one-dimensional domain in axisymmetric problems. A marching method is then used to move forward in the axial direction of the microchannel. The pressure–velocity coupling is dealt with using an improved projection algorithm already employed by one of the authors (C.N.) for the solution of the Navier–Stokes equations in their elliptic form (Nonino, 2003).

Most of the features of the adopted solution algorithm and of the finite element discretization procedure can be found in Nonino et al. (1988), where reference is made to a constant property fluid and to the dimensionless forms of the governing equations. Since this description can be easily adapted to the case of a fluid with temperature dependent properties considered here, only the details concerning the estimation of the average pressure gradient $\mathrm{d}\bar{p}/\mathrm{d}x$, which is necessary to solve the momentum equation in the axial direction, are reported in this paper. With reference to the flow in straight ducts, integration of the axial momentum equation over the cross-section A gives (Shah and London, 1978; Nonino et al., 1988)

$$-\frac{\mathrm{d}\bar{p}}{\mathrm{d}x}=\frac{\mathrm{d}}{\mathrm{d}x}\left(\frac{1}{A}\int_{\mathrm{A}}\rho u^2\mathrm{d}A\right)-\frac{1}{A}\int_P\mu\frac{\partial u}{\partial n}\mathrm{d}P=\frac{\mathrm{d}K}{\mathrm{d}x}+L \tag{12}$$

In the previous equation P is the perimeter of the cross-section and n denotes the direction of the outer normal to the boundary, while of K and L represent the axial momentum rate and the wall viscous force per unit length, respectively, referred to the unit area of the cross-section. Their definitions can be directly inferred from the above equation. In the marching procedure from the nth to the $(n+1)$th axial locations, the following approximation for the average pressure gradient is used

$$-\left(\frac{\mathrm{d}\bar{p}}{\mathrm{d}x}\right)^*=\left(\frac{\mathrm{d}K}{\mathrm{d}x}\right)^*+L^n=\frac{1}{2}\left(\frac{K^n-K^{n-1}}{x^n-x^{n-1}}+\frac{K^n-K^{n-2}}{x^n-x^{n-2}}\right)+L^n \tag{13}$$

where the asterisk (*) indicates an estimated value. The backward formula employed in Eq. (13) for the evaluation of $(dK/dx)^*$ has been adopted to increase stability since we observed that more accurate second order approximations very often led to the divergence of the simulations. However, it must be pointed out that this choice does not affect the overall accuracy of the numerical results if, as will be detailed later, very small axial steps are adopted where the variations of the axial pressure gradient are significant, that is, in the region very close to the duct entrance.

3. Numerical results

The laminar forced convection in the heated/cooled part of straight microchannels of constant cross-sections with uniform wall temperature t_w is studied in this paper. The hypotheses made here are that viscous dissipation effects are not negligible and that viscosity varies with temperature, while all the other thermophysical properties are constant. As already pointed out in the Introduction, in many cases, fluid velocity and temperature fields in microchannels do not develop simultaneously, resulting in non-overlapping hydrodynamic and thermal entrance regions. A broad range of situations of practical interest can be described with reference to the scheme reported in Fig. 1, where it is assumed that the fluid enters the microchannel at uniform velocity u_e and temperature t_e, and that the walls of the first part (of length L_0) of the duct are maintained at the same temperature t_e. Then, the wall temperature exhibits a step change from t_e to t_w at the axial position where liquid heating/cooling begins ($x = 0$). The two limiting situations are considered here: (i) thermally developing and hydrodynamically fully developed flow and (ii) simultaneously developing flow. In the first case, L_0 is larger than the axial distance necessary to allow the flow to reach fully developed conditions. Therefore, because of viscous heating, at the entrance of the heated/cooled part of the microchannel a non-uniform distribution of temperature t is obtained, with $t - t_e > 0$ everywhere on the cross-section, except on the contour, where $t - t_e = 0$. This causes a viscosity variation over the cross-section, which, in turn, influences the velocity profile. As a consequence, for each combination of cross-sectional geometry, characteristics of viscosity variations with temperature and Brinkman number, the appropriate velocity and temperature distributions to be specified as inlet conditions at $x = 0$ have been determined by means of preliminary numerical simulations. It must be pointed out that the alternative assumption that the first part of the microchannel is adiabatic would make the problem undetermined. In fact, in such a case, due to the combined effects of viscous heating and temperature dependent viscosity, the length L_0 would always influence temperature and velocity profiles at the axial position where fluid heating/cooling begins, and the flow could not reach fully developed conditions, no matter how large L_0 is. Instead, in the second case, i.e., in simultaneously developing flows, fluid heating/cooling begins at the microchannel inlet, where the velocity field also starts to develop. This means that L_0 is equal to 0 and that the liquid enters the channel with a uniform temperature t_e and a uniform velocity u_e equal to the average axial velocity $\bar{u}$.

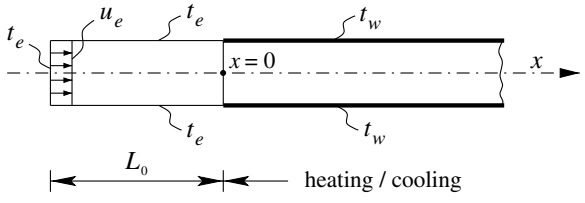

Fig. 1. General scheme for the application of thermal boundary conditions.

The dynamic viscosity is assumed to vary with temperature and μ_e and μ_w are its values at t_e and t_w, respectively. The ratio of μ_e over μ_w gives an indication of the relevance of the temperature dependence of viscosity in the range between t_e and t_w. While it is true that exponential (or modified Arrhenius type) relations are usually employed to represent the temperature dependence of viscosity, the linear variation (Berardi and Cuccurullo, 2000; Sahin, 1999) adopted in this paper is much simpler to deal with in the context of a systematic study and represents an acceptable approximation if the ratio of maximum to minimum values of viscosity is not too large. To strengthen this argument, we show in Fig. 2 the graphical representation of the linear relation

$$\mu = \mu_w + \alpha(t - t_w) \tag{14}$$

and of a widely used exponential formula (Kakaç, 1987)

$$\mu = \mu_w \exp[-\beta(t - t_w)] \tag{15}$$

for the values of μ_e/μ_w in the range between 1/2 and 2 considered in this paper. In Eqs. (14) and (15), α and β are

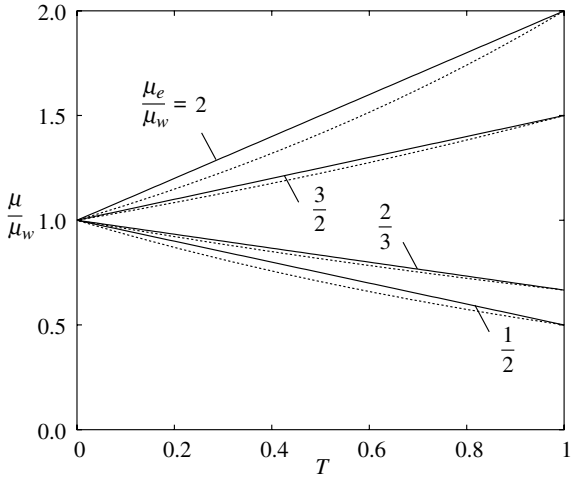

Fig. 2. Graphical representation of linear and exponential viscosity–temperature relations for different values of μ_e/μ_w. Solid lines: linear relation; dotted lines: exponential relation.

parameters defined as $\alpha = (\mu_e - \mu_w)/(t_e - t_w)$ and $\beta = -(d\mu/dt)/\mu = \text{const.}$, respectively, while the dimensionless temperature appearing in Fig. 2 is defined as $T = (t - t_w)/(t_e - t_w)$. As can be seen, the linear relation represents a reasonably good approximation of the exponential one for the values of μ_e/μ_w considered here.

It is worth noting that, since all the other thermophysical properties are assumed constant, we have $\mu_e/\mu_w = Pr_e/Pr_w = Re_w/Re_e$. Moreover, while the local Reynolds number $Re = \rho\bar{u}D_h/\mu$ and the local Prandtl number $Pr = \mu c/k$ depend on temperature, the local Péclet number $Pe = RePr = Re_e\ Pr_e = Re_w\ Pr_w$ always has the same value. As the viscosity of liquids decreases with increasing temperature, $Pr_e/Pr_w > 1$ corresponds to fluid heating ($t_e < t_w$) and $Pr_e/Pr_w < 1$ to fluid cooling ($t_e > t_w$), while $Pr_e/Pr_w = 1$ refers to isothermal flows ($t_e = t_w$) or to constant viscosity fluids. The reference Brinkman number $Br_m = \mu_m\bar{u}^2/[k(t_e - t_w)]$ is negative for fluid heating and positive for fluid cooling. In all the computations, the same values $Re_m = \rho\bar{u}D_h/\mu_m = 500$ and $Pr_m = \mu_m\, c/k = 5$ of the Reynolds and Prandtl numbers at the reference temperature of the fluid $t_m = (t_e + t_w)/2$ have been assumed. The corresponding value of the Péclet number Pe is 2500. Therefore, for the values of the ratio $Pr_e/Pr_w = 1/2, 2/3, 1, 3/2$ and 2 considered here, minimum and maximum values of the local Reynolds number in the temperature range between t_e and t_w are 375 and 750, respectively, while the Prandtl number can vary between $3.\bar{3}$ and $6.\bar{6}$. In addition to $Br_m = 0$, corresponding to negligible viscous dissipation, reasonable non-zero values of the reference Brinkman number have been selected, namely, $Br_m = \pm 0.001$, ± 0.01 and ± 0.1. In the following, numerical results concerning axial distributions of the local Nusselt number $Nu = h\ D_h/k$ and of the apparent Fanning friction factor f_a are presented. The local convection coefficient h, averaged over the heated/cooled perimeter of the cross-section, can be computed as

$$h = \frac{q'_w}{P_t(t_b - t_w)} \tag{16}$$

for three-dimensional geometries, and as

$$h = \frac{q''_w}{t_b - t_w} \tag{17}$$

for axisymmetric geometries. In the above equations, q'_w and q''_w are the wall heat transfer rate per unit length and the wall heat flux, respectively, P_t is the heated/cooled perimeter of the cross-section and t_b is the bulk temperature. The apparent Fanning friction factor is defined as (Shah and London, 1978)

$$f_a = \frac{(\bar{p}_e - \bar{p})D_h}{2\rho\bar{u}^2 x} \tag{18}$$

It must be pointed out that, even if the numerical results reported in the following have been obtained for $Re_m = 500$ and $Pr_m = 5$, they are much more general that what they appear to be. In fact, for a given reference Prandtl number Pr_m, the axial distributions of Nu and $f_a\ Re_m$ are independent of the reference Reynolds number Re_m, provided that the appropriate dimensionless axial coordinates $X^* = x/D_hPe$ and $X^+ = x/D_hRe_m$ are employed. Moreover, the influence of the reference Prandlt number Pr_m on Nu and f_aRe_m distributions is significant only in the first part of the microchannel, i.e., near the entrance. The validity of the above statements, which is well established for constant property fluids, has been verified, by means of sample numerical tests, also under the variable viscosity assumption in the ranges $1/2 \leqslant \mu_e/\mu_w \leqslant 2$, $250 \leqslant Re_m \leqslant 1000$ and $2 \leqslant Pr_m \leqslant 20$.

Three different cross-sectional geometries are considered in this study, namely circular, rectangular with aspect ratio $\gamma = a/b = 0$ (parallel plate channel) and trapezoidal with $\gamma = a/b = 0.414$; the latter corresponds to an isosceles trapezium with the larger base b and height a and a 54.74° angle between sides and larger base (Morini, 2005b; Nonino et al., 2005b). Computational domains have been defined taking into account existing symmetries. Therefore, the circular cross-section corresponds to a one-dimensional axisymmetric domain of length r_o, the rectangular cross-section with $\gamma = 0$ to a rectangle of unit base and height $a/2$, and the trapezoidal cross-section to the two-dimensional domain of larger base $b/2$ and height a, equal to one half of the whole cross-section. One-dimensional domains have been discretized by means of three-node parabolic elements, while two-dimensional ones have been subdivided into 9-node Lagrangian parabolic elements. A total of 50 elements and 101 nodal points have been used in the discretization of the 1-D domain corresponding to the circular cross-section, and a total of 50 elements and 303 nodal points in that of the 2-D domain corresponding to the rectangular cross-section with $\gamma = 0$. Instead, to give comparably accurate results, a mesh of 12,000 elements and 48,441 nodal points has been used for the trapezoidal cross-section. Element sizes gradually increase with increasing distance from the walls. The minimum and maximum values of the dimensionless distances between adjacent nodes $\Delta y/D_h$ and $\Delta z/D_h$, or $\Delta r/D_h$, measured in the transverse or in the radial directions, respectively, are reported in Table 1 for the three cross-sectional geometries considered. The adopted meshes are fine enough near the walls to allow an accurate representation of the steep velocity and temperature gradients taking place there as the flow develops. Of course, preliminary tests had been carried out to verify that all these discretizations are fine enough to give mesh-independent results. In all the computations, the axial step has gradually been increased from the starting value $\Delta x/D_h = 0.0001$ to the maximum value $\Delta x/D_h = 0.05$. As the initial value of the axial step is very small, the strong variations of the axial pressure gradient arising in the first part of the microchannel can be adequately captured.

3.1. Validation of the procedure

The procedure outlined in the previous section and employed for the numerical simulations has already been validated, on the assumptions of constant property fluid

Table 1
Minimum and maximum values of the dimensionless distances between adjacent nodes $\Delta y/D_h$ and $\Delta z/D_h$, or $\Delta r/D_h$, in the finite element meshes employed for the numerical simulations

Cross-section	$\Delta y_{min}/D_h$ or $\Delta r_{min}/D_h$	$\Delta z_{min}/D_h$	$\Delta y_{max}/D_h$ or $\Delta r_{max}/D_h$	$\Delta z_{max}/D_h$
Circular	0.0002	–	0.0082	–
Parallel plates	0.0001	–	0.0041	–
Trapezoidal	0.0002	0.0001	0.0070	0.0063

and negligible viscous dissipation, by comparing heat transfer and pressure drop results with existing literature data for laminar simultaneously developing flows in straight channels, both three-dimensional and axisymmetric (Nonino et al., 1988; Nonino et al., 2005a; Nonino et al., 2005b). In order to assess the accuracy of the present computations, additional validation tests have been carried out. Asymptotic values of the Nusselt number $(Nu_\infty)_c$ and fully developed values of the Poiseuille number $(fRe)_c$ for a constant property fluid are compared here with available literature data. For circular microchannels, the computed values $(Nu_\infty)_c = 3.65680$ and 9.60000 for $Br = 0$ and $Br \neq 0$, respectively, are in excellent agreement with the corresponding literature values $(Nu_\infty)_c = 3.65679$ and $48/5 = 9.6$ (Shah and London, 1978; Barletta, 1997; Zanchini, 1997). The same result is obtained for parallel plate microchannels with negligible viscous dissipation, for which the computed and the literature values are $(Nu_\infty)_c = 7.54075$ and 7.54070, respectively (Shah and London, 1978). Computed fully developed values of the Poiseuille number $(fRe)_c = 16.0000$, 24.0000 and 14.0555 for circular, parallel plate and trapezoidal microchannels, respectively, are almost coincident with the corresponding literature values $(fRe)_c = 16$, 24 and 14.053 (Shah and London, 1978; Morini, 2005b). Moreover, the procedure is also validated here on the assumption of non-negligible viscous dissipation, with reference to thermally developing and hydrodynamically fully developed flows of constant property fluids in circular ducts, for which an analytical solution exists (Basu and Roy, 1985).

As in Basu and Roy (1985), a fully developed (parabolic) axial velocity profile $u = 2\bar{u}[1 - (r/r_o)^2]$ and a uniform temperature profile $t = t_e$ are assumed at the inlet of a circular duct of outer radius r_o, while a uniform temperature t_w is imposed at the duct wall. The axial velocity profile is assumed to remain the same along the whole duct length, while, due to heat transfer and viscous dissipation, the temperature profile changes with the axial position until thermally developed flow conditions are reached. In our calculations, fluid properties and flow parameters are assumed to yield the values $Re = 500$ and $Pr = 5$ of the Reynolds and Prandtl numbers, respectively. Three values of the Brinkman number $Br = 0.001$, 0.1 and 1 are considered here among those of Basu and Roy (1985), to account for reasonable viscous dissipation effects. Axial distributions of computed Nusselt number Nu_c are always in very good agreement with the analytical results of Basu and Roy (1985), as can be seen in Fig. 3.

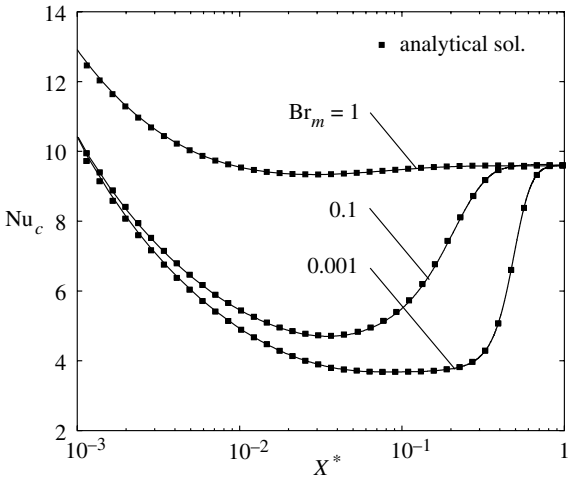

Fig. 3. Thermally developing and hydrodynamically fully developed flows in circular ducts: comparisons of numerical results (solid lines) with analytical solutions by Basu and Roy (1985) for different values of the Brinkman number.

Finally, axial distributions of computed $(f_aRe)_c$ for developing constant property flows in circular and parallel plate ducts are compared in Fig. 4 with available literature data from Shah and London (1978). The distribution of $(f_aRe)_c$ for flows in the trapezoidal ducts considered in this paper, for which no comparison data are available in the literature, is also reported in Fig. 4 for the sake of completeness.

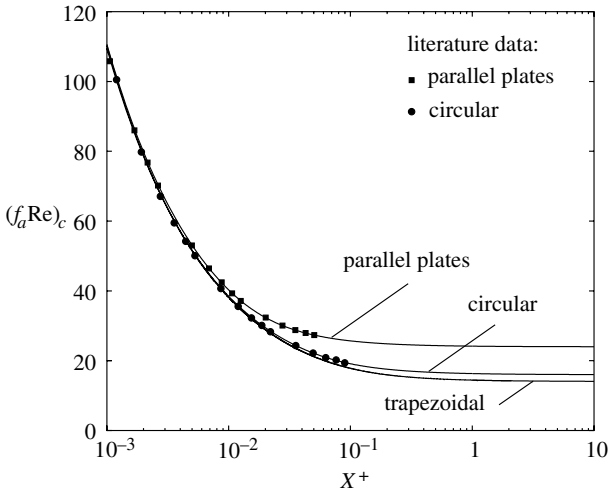

Fig. 4. Axial distributions of $(f_aRe)_c$ for developing constant property flows in microchannels of different cross-sections: comparisons of numerical results (solid lines) with literature data (Shah and London, 1978).

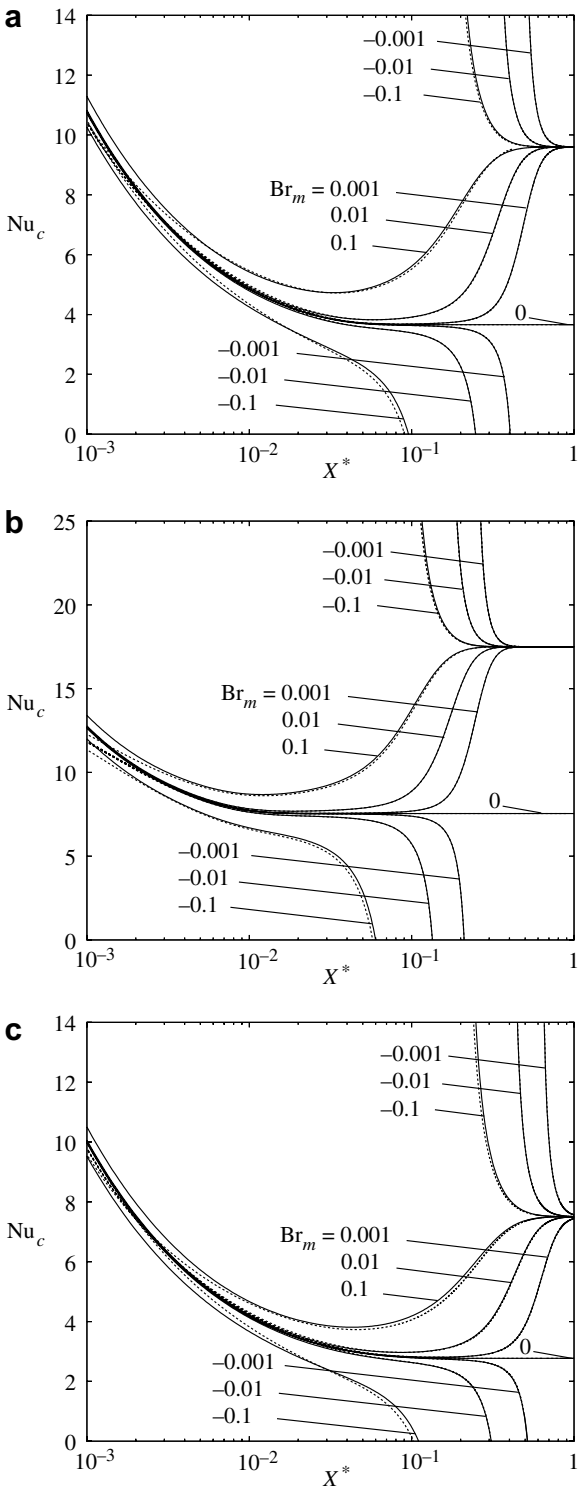

Fig. 5. Axial distributions of the Nusselt number Nu_c for constant property flows with $Pr_m = 5$ and different Brinkman numbers Br_m: (a) circular cross-section, (b) rectangular cross-section with $\gamma = 0$ (parallel plates) and (c) trapezoidal cross-section with $\gamma = 0.414$. Solid lines: simultaneously developing flows; dotted lines: thermally developing flows.

3.2. Heat transfer results

The influence of viscous dissipation on the local Nusselt number is illustrated in Fig. 5, where numerical results concerning axial distributions of Nu_c for constant property flows ($Pr_e/Pr_w = 1$) with different Brinkman numbers are presented for both thermally developing flows and simultaneously developing flows. As expected, for a given cross-sectional geometry, the same asymptotic value $(Nu_\infty)_c$ is reached for fully developed conditions with any non-zero value of Br_m, both in thermally developing flows and in simultaneously developing flows, while Br_m strongly affects the Nusselt number in the intermediate range of X^*. The influence of Br_m is also significant for very low values of X^*, where, for simultaneously developing flows, the values of Nu_c are always lower than those corresponding to $Br_m = 0$ if $Br_m < 0$ (fluid heating), and higher if $Br_m > 0$ (fluid cooling). For thermally developing flows in microchannels of circular and trapezoidal cross-sections, the curves for $Br_m \neq 0$ cross each other and the one for $Br_m = 0$. As expected, for all the geometries the curves pertaining to thermally developing flows with $Br_m = 0$ lie under the corresponding ones for simultaneously developing flows, while, because of the above mentioned curve crossing, this is not always true for $Br_m \neq 0$.

The effects of temperature dependent viscosity on the local Nusselt number are illustrated in Figs. 6–8, where axial distributions of the ratio Nu/Nu_c for microchannels of different cross-sections are presented. As can be seen, the ratio Pr_e/Pr_w significantly affects the Nusselt number as long as the flow develops, while its influence is rather small when fully developed conditions are reached. Obviously, in the first part of the microchannel the differences between the results obtained for thermally developing flows and for simultaneously developing flows are also more appreciable. For very low values of X^*, the curves of Nu/Nu_c are nearly horizontal, at least for circular and trapezoidal cross-sections, and exhibit deviations from unity larger for thermally developing flows than for simultaneously developing flows. Then, for intermediate values of X^*, except for the case of fluid heating ($Pr_e/Pr_w > 1$) with $|Br_m| = 0.1$, all the curves tend to converge towards unity. It must be observed that the very high values of the ratio Nu/Nu_c found at intermediate X^* for heating are not very significant, since they are simply due to a moderate axial shifting of curves representing axial distributions of Nu with respect to the constant property ones reported in Fig. 5. By comparing the axial distributions of Nu/Nu_c for the same cross-sectional geometry, but for different Brinkman numbers Br_m, it can be seen that, both in thermally developing flows and in simultaneously developing flows, the influence of temperature dependent viscosity is more evident than the one due to viscous dissipation.

Moreover, for a given $|Br_m|$, liquid heating ($Br_m < 0$ and $Pr_e/Pr_w > 1$) and liquid cooling ($Br_m > 0$ and $Pr_e/Pr_w < 1$) lead to the same asymptotic value of the ratio Nu/Nu_c provided that the corresponding values of the ratio Pr_e/Pr_w are reciprocal to each other, i.e., the liquid exhibits the same variation of viscosity in the temperature range between t_e

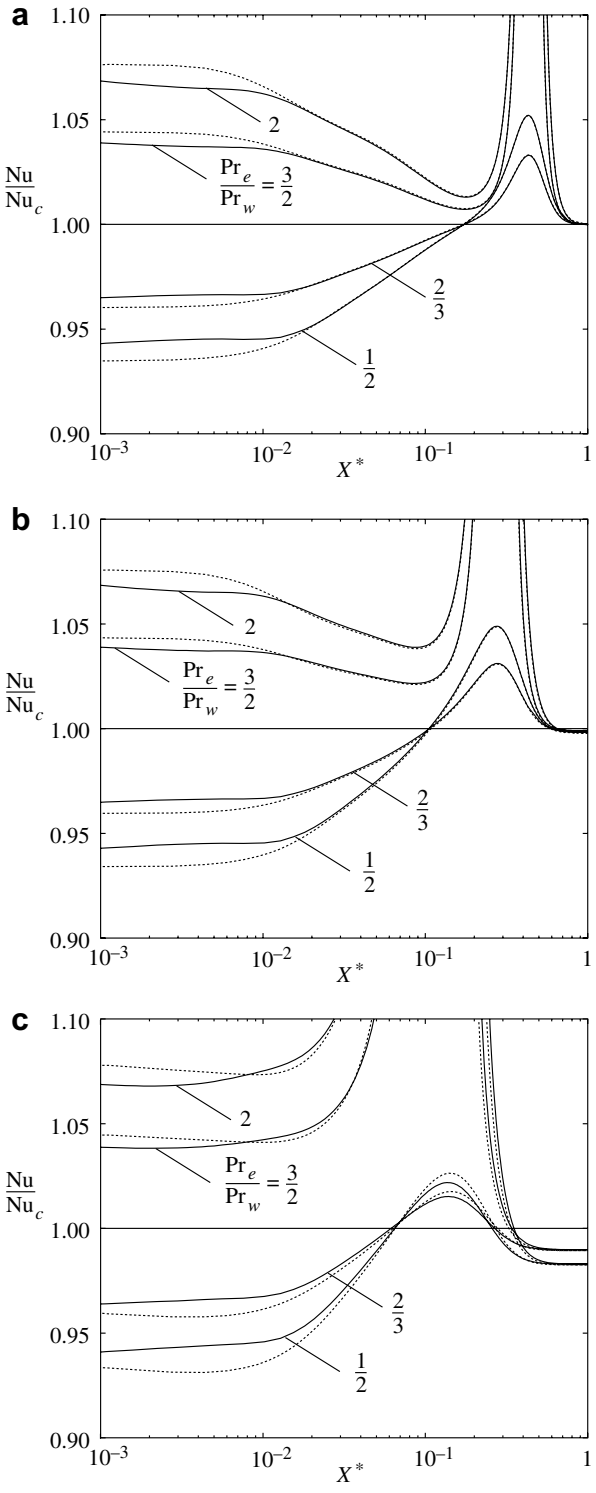

Fig. 6. Axial distributions of the ratio Nu/Nu_c for microchannels of circular cross-section: (a) $|Br_m| = 0.001$, (b) $|Br_m| = 0.01$ and (c) $|Br_m| = 0.1$. Solid line: simultaneously developing flows; dotted lines: thermally developing flows.

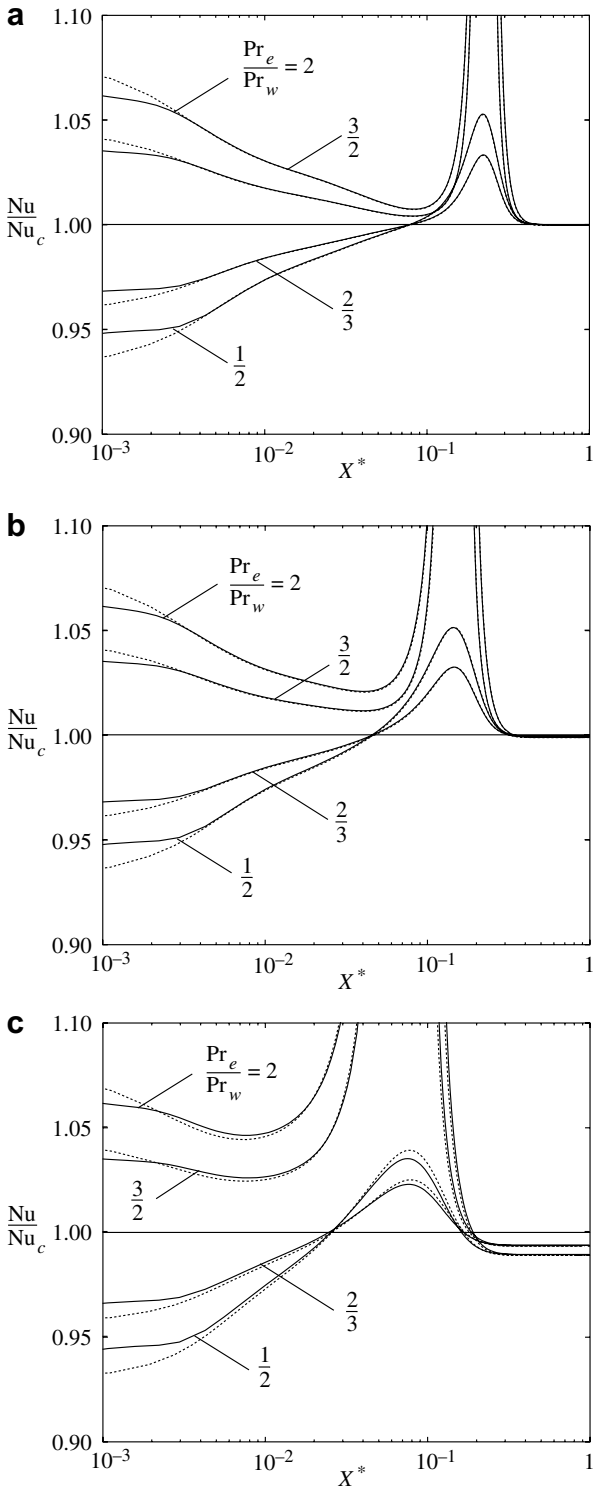

Fig. 7. Axial distributions of the ratio Nu/Nu_c for microchannels of rectangular cross-section with $\gamma = 0$ (parallel plates): (a) $|Br_m| = 0.001$, (b) $|Br_m| = 0.01$ and (c) $|Br_m| = 0.1$. Solid lines: simultaneously developing flows; dotted lines: thermally developing flows.

and t_w. On the basis of Eqs. (16) and (17), this implies that fully developed profiles of the absolute values of the dimensionless temperature $T'_\infty = [(t - t_w)/(t_b - t_w)]_\infty$ are the same for both heating and cooling. This also implies that fully developed profiles of the axial velocity are equal for liquid heating and liquid cooling, so that the term Φ_v, defined in Eqs. (6) and (11), has the same distribution over the cross-section in both cases.

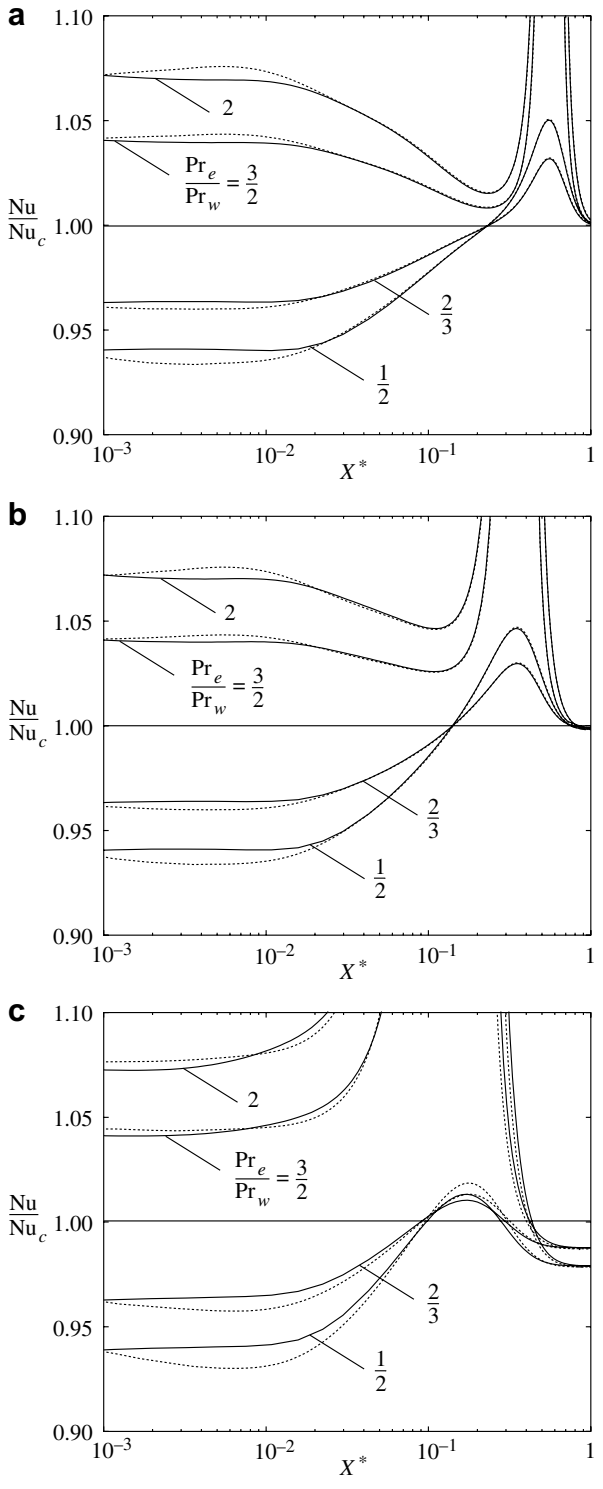

Fig. 8. Axial distributions of the ratio Nu/Nu_c for microchannels of trapezoidal cross-section with $\gamma = 0.414$: (a) $|Br_m| = 0.001$, (b) $|Br_m| = 0.01$ and (c) $|Br_m| = 0.1$. Solid lines: simultaneously developing flows; dotted lines: thermally developing flows.

3.3. Pressure drop results

The combined effects of temperature dependent viscosity and of viscous dissipation on pressure drop are illustrated in Figs. 9–11 for both thermally developing flows and simultaneously developing flows with different values of Br_m and of Pr_e/Pr_w. In these figures, axial distributions of the ratio $f_aRe_m/(f_aRe_m)_c$ are reported for the three cross-sectional geometries considered. It must be pointed out that, for thermally developing flows of constant property fluids, $(f_aRe_m)_c$ coincides with $(fRe)_c$, since there is no evolution of the velocity profile along the heated/cooled part of the duct. For all the geometries considered here, the values of $(fRe)_c$ have already been reported in subsection 3.1, while axial distributions of $(f_aRe_m)_c$, coincident with $(f_aRe)_c$, for developing flows have been presented in Fig. 4. It is apparent in Figs. 9–11 that, as expected, $f_aRe_m/(f_aRe_m)_c$ is always larger than 1 for fluid cooling ($Pr_e/Pr_w < 1$ and $Br_m > 0$) and smaller than 1 for fluid heating ($Pr_e/Pr_w > 1$ and $Br_m < 0$). In fact, in the first case the pressure drop is higher than the one corresponding to the flow of a constant property fluid, due to the higher values of viscosity in the near wall region ($\mu_w > \mu_m$), while the opposite occurs in the second case ($\mu_w < \mu_m$). For each combination of Br_m and Pr_e/Pr_w, the curves for thermally

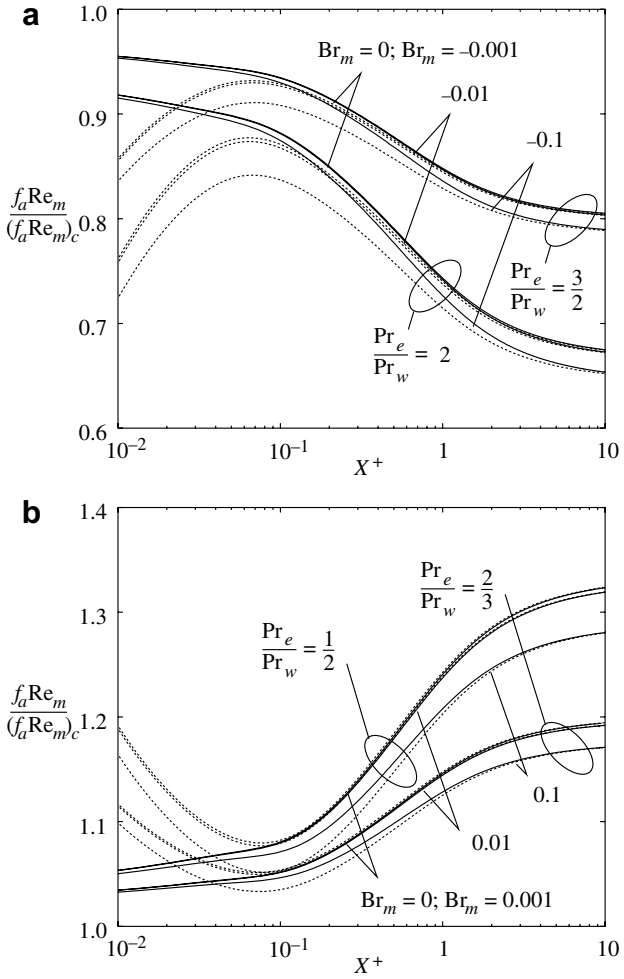

Fig. 9. Axial distributions of the ratio $f_aRe_m/(fRe_m)_c$ for microchannels of circular cross-section: (a) heating, (b) cooling. Solid lines: simultaneously developing flows; dotted lines: thermally developing flows.

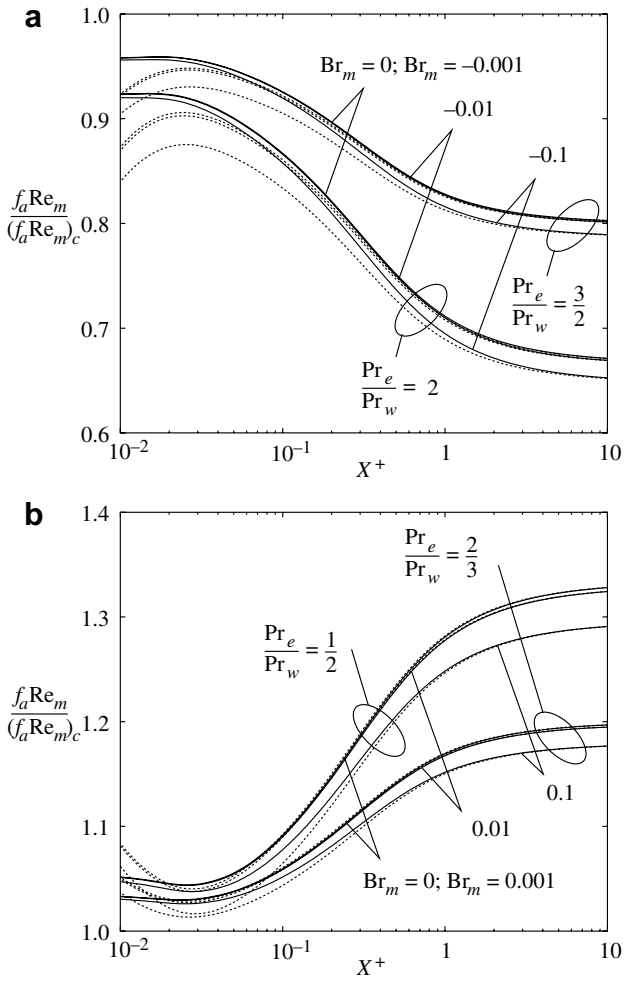

Fig. 10. Axial distributions of the ratio $f_a Re_m/(fRe_m)_c$ for microchannels of rectangular cross-section with $\gamma = 0$ (parallel plates): (a) heating, (b) cooling. Solid lines: simultaneously developing flows; dotted lines: thermally developing flows.

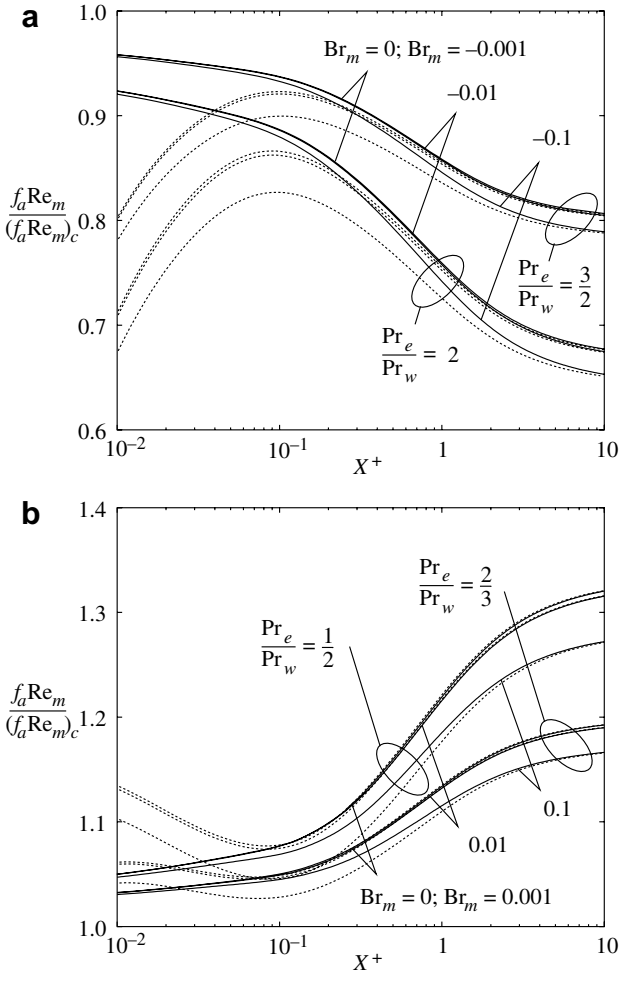

Fig. 11. Axial distributions of the ratio $f_a Re_m/(fRe_m)_c$ for microchannels of trapezoidal cross-section with $\gamma = 0.414$: (a) heating, (b) cooling. Solid lines: simultaneously developing flows; dotted lines: thermally developing flows.

developing flows and those pertaining to simultaneously developing flows approach the same asymptotic value since, far enough from the microchannel entrance, velocity and temperature profiles are the same, independently of the inlet conditions. Moreover, asymptotic values $[f_a Re_m/(f_a Re_m)_c]_\infty$ of the ratio $f_a Re_m/(f_a Re_m)_c$ for $Br = 0$ only depend on Pr_e/Pr_w, no matter which cross-sectional geometry is considered. In fact, we can write

$$\left[\frac{f_a Re_m}{(f_a Re_m)_c}\right]_\infty = \frac{fRe_m}{(fRe)_c} = \frac{fRe_w}{(fRe)_c}\frac{\mu_w}{\mu_m} = \frac{\mu_w}{\mu_m} = \frac{Pr_w}{Pr_m} \tag{19}$$

since it is $fRe_w = (fRe)_c = C$, where C is a constant whose value depends on the particular cross-sectional geometry considered (Shah and London, 1978). Therefore, the asymptotic values $[f_a Re_m/(f_a Re_m)_c]_\infty = 1.\bar{3}$, 1.2, 0.8 and $0.\bar{6}$ are obtained for $Pr_e/Pr_w = 1/2$, 2/3, 3/2 and 2, respectively, as shown in Figs. 9–11. Instead, for low values of X^+, the curves of the ratio $f_a Re_m/(f_a Re_m)_c$ for thermally developing flows and simultaneously developing flows diverge, with the first one showing larger deviations from unity. This can be justified considering that, in thermally developing flows, only temperature dependent viscosity and viscous dissipation are responsible for the deviations of temperature and velocity distributions from those obtained with constant property fluids, while, in simultaneously developing flows, their effects are marginal if compared with those related to the evolution of the velocity profile from uniform inlet conditions.

3.4. Velocity and temperature profiles

The differences between the local values of Nu/Nu_c and $f_a Re_m/(f_a Re_m)_c$ found for different values of the ratio Pr_e/Pr_w can be explained taking into account velocity and temperature distributions over the cross-sections. As an example, to show the effects of temperature dependent viscosity, radial profiles of the dimensionless axial velocity $U = u/\bar{u}$ at selected axial locations are reported in Fig. 12(a) for flows in circular microchannels with different values of Pr_e/Pr_w and $|Br_m| = 0.1$. Instead, to show the influence of

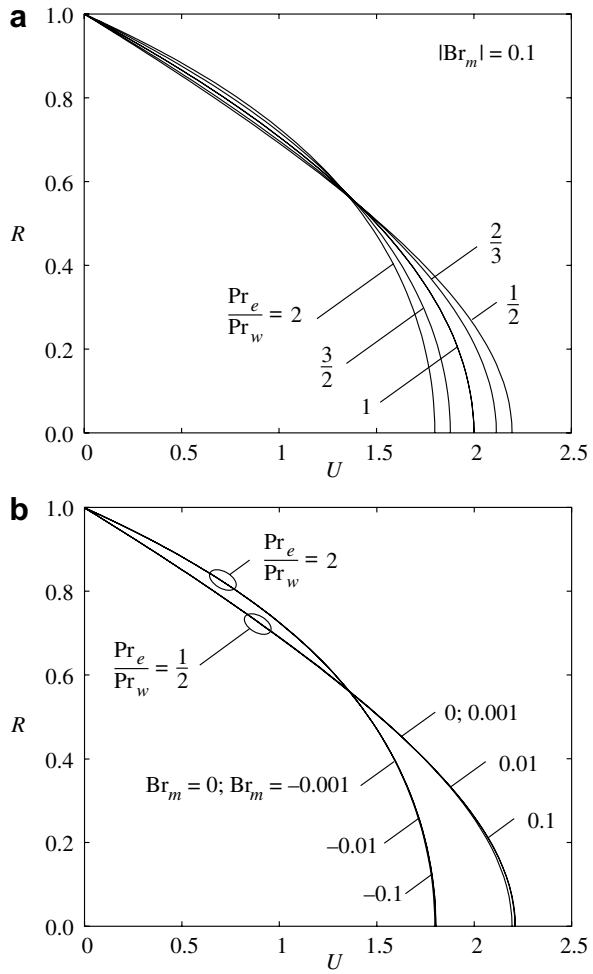

Fig. 12. Radial profiles of dimensionless velocity U at the axial positions where $T_b = 0.5$ for simultaneously developing flows in ducts of circular cross-section for $Pr_m = 5$: (a) effect of the temperature dependent viscosity and (b) effect of the Brinkman number.

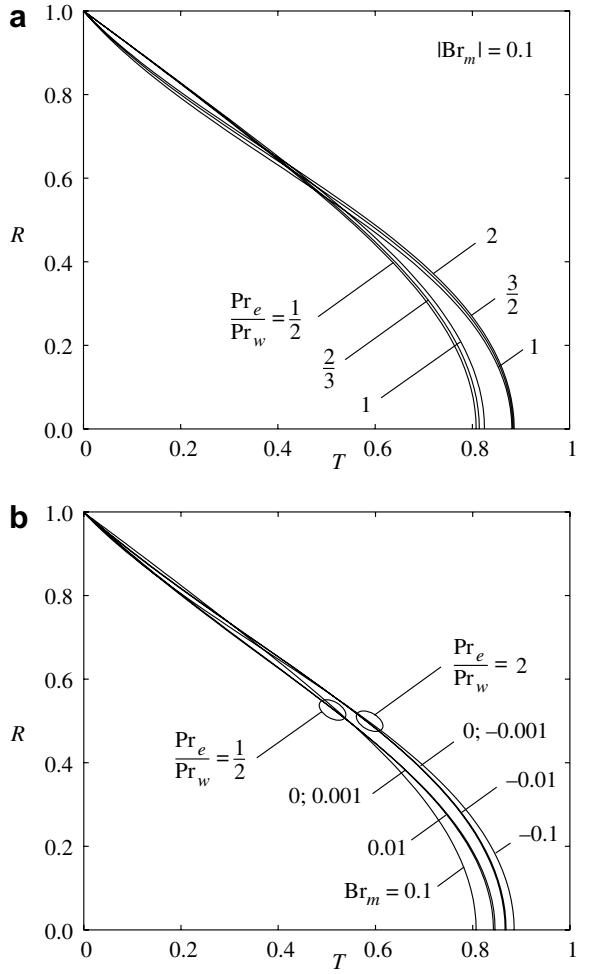

Fig. 13. Radial profiles of dimensionless temperature T at the axial positions where $T_b = 0.5$ for simultaneously developing flows in ducts of circular cross-section for $Pr_m = 5$: (a) effect of the temperature dependent viscosity and (b) effect of the Brinkman number.

viscous heating, the distributions of U are reported in Fig. 12(b) for $Pr_e/Pr_w = 2$ (fluid heating) and $Pr_e/Pr_w = 1/2$ (fluid cooling) and for all the Brinkman numbers considered here. Similarly, the profiles of the dimensionless temperature $T = (t - t_w)/(t_e - t_w)$ at the same axial locations and for the same cross-sectional geometry are reported in Fig. 13(a) for the considered values of Pr_e/Pr_w and $|Br_m| = 0.1$ and in Fig. 13(b) for $Pr_e/Pr_w = 2$ (fluid heating) and $Pr_e/Pr_w = 1/2$ (fluid cooling) and for different Brinkman numbers. In order to consider comparable situations, the dimensionless velocity and temperature profiles reported in Figs. 12 and 13 refer to axial locations where the bulk temperature t_b coincides with the reference temperature of the fluid t_m, so that $T_b = (t_b - t_w)/(t_e - t_w) = 0.5$. From Figs. 12(a) and 13(a) it is apparent that the temperature dependence of viscosity has an important effect on the velocity distribution but a rather weak one on the temperature profile. On the contrary, as can be seen in Figs. 12(b) and 13(b), viscous heating has an influence that is significant on the temperature field, but negligible on the velocity distribution. The explanation can be found considering that temperature differences over the cross-section of the channel caused by the application of wall thermal boundary conditions are much larger that the local temperature differences produced by viscous heating.

4. Conclusions

The effects of viscous dissipation and temperature dependent viscosity both in thermally developing and hydrodynamically fully developed flows and in simultaneously developing flows of liquids in straight microchannels of arbitrary but constant cross-sections have been studied. In order to allow a parametric investigation, viscosity has been assumed to vary linearly with temperature, while the other fluid properties have been held constant. Different cross-sectional geometries have been considered, chosen among those usually adopted for microchannels, namely circular, rectangular with aspect ratio $\gamma = 0$ (parallel plate channel) and trapezoidal with $\gamma = 0.414$. Reference has been made

to uniform wall temperature boundary conditions. Numerical results confirm that, in the laminar forced convection in straight microchannels, both temperature dependence of viscosity and viscous dissipation effects cannot be neglected in a wide range of operative conditions.

Acknowledgement

This work was funded by MIUR (PRIN/COFIN 2003 and 2005 projects).

References

Barletta, A., 1997. Fully developed laminar forced convection in circular ducts for power-law fluids with viscous dissipation. Int. J. Heat Mass Transfer 40, 15–26.

Basu, T., Roy, D.N., 1985. Laminar heat transfer in a tube with viscous dissipation. Int. J. Heat Mass Transfer 28, 699–701.

Berardi, P.G., Cuccurullo, G., 2000. The effects of variable properties on velocity and temperature fields in the entrance region of pipe flow. In: Proc. of the 55th ATI National Conference, Bari, Italy.

Cuccurullo, G., Berardi, P.G., 2000. Temperature field for developing pipe flow of non-Newtonian fluids with viscous heating. In: Proc. of the 18th UIT National Conference, Cernobbio, Italy, pp. 107–117.

Herwig, H., Hausner, O., 2003. Critical view on new results in microfluid mechanics: an example. Int. J. Heat Mass Transfer 46, 935–937.

Hirsh, C., 1988. Numerical Computation of Internal and External Flows, Vol. 1. Wiley, New York, p. 70.

Javeri, V., 1977. Heat transfer in laminar entrance region of a flat channel for the temperature boundary condition of the third kind. Wärme- und Stoffübertragung 10, 137–144.

Kakaç, S., 1987. The effect of temperature-dependent fluid properties on convective heat transfer. In: Kakaç, S., Shah, R.K., Aung, W. (Eds.), Handbook of Single-Phase Convective Heat Transfer. Wiley, New York (Chapter 18).

Koo, J., Kleinstreuer, C., 2003. Liquid flow in microchannels: experimental observations and computational analyses of microfluids effects. J. Micromech. Microeng. 13, 568–579.

Koo, J., Kleinstreuer, C., 2004a. Viscous dissipation effects in microtubes and microchannels. Int. J. Heat Mass Transfer 47, 3159–3169.

Koo, J., Kleinstreuer, C., 2004b. Analysis of liquid flow in microconduits. In: Proc. of the 2nd ICMM, Rochester (NY), pp. 191–198.

Lin, T.F., Hawks, K.H., Leidenfrost, W., 1983. Analysis of viscous dissipation effect on thermal entrance heat transfer in laminar pipe flows with convective boundary conditions. Wärme- und Stoffübertragung 17, 97–105.

Morini, G.L., 2005a. Viscous dissipation as scaling effect for liquid flows in microchannels. In: Proc. of the 3rd ICMM, Toronto, Canada.

Morini, G.L., 2005b. Viscous heating in liquid flows in microchannels. Int. J. Heat Mass Transfer 48, 3637–3647.

Nóbrega, J.M., Pinho, F.T., Oliveira, P.J., Carneiro, O.S., 2004. Accounting for temperature dependent properties in viscoelastic duct flows. Int. J. Heat Mass Transfer 47, 1141–1158.

Nonino, C., 2003. A simple pressure stabilization for a SIMPLE-like equal-order FEM algorithm. Numer. Heat Transfer, Part B 44, 61–81.

Nonino, C., Del Giudice, S., Comini, G., 1988. Laminar forced convection in three-dimensional duct flows. Numer. Heat Transfer 13, 451–466.

Nonino, C., Del Giudice, S., Savino, S., 2005a. Influence of temperature dependent viscosity in laminar forced convection in axisymmetric straight ducts (in Italian). In: Proc. of the 23rd UIT National Conference, Parma, Italy, pp. 323–328.

Nonino, C., Del Giudice, S., Savino, S., 2005b. Influence of temperature dependent viscosity in laminar forced convection in microchannels (in Italian). In: Proc. of the 23rd UIT National Conference, Parma, Italy, pp. 329–334.

Nouar, C., 1999. Numerical solution for laminar mixed convection in a horizontal annular duct: temperature-dependent viscosity effect. Int. J. Numer. Methods Fluids 29, 849–864.

Patankar, S.V., Spalding, D.B., 1972. A calculation procedure for heat, mass and momentum transfer in three-dimensional parabolic flows. Int. J. Heat Mass Transfer 15, 1787–1806.

Sahin, A.Z., 1999. The effect of variable viscosity on the entropy generation and pumping power in a laminar fluid flow through a duct subjected to constant heat flux. Heat Mass Transfer 35, 499–506.

Shah, R.K., Bhatti, M.S., 1987. Laminar convective heat transfer in ducts. In: Kakaç, S., Shah, R.K., Aung, W. (Eds.), Handbook of Single-Phase Convective Heat Transfer. Wiley, New York (Chapter 3).

Shah, R.K., London, A.L., 1978. Laminar Flow Forced Convection in Ducts. Academic Press, New York.

Shen, P., Aliabadi, S.K., Abedi, J., 2004. A review of single-phase liquid flow and heat transfer in microchannels. In: Proc. of the 2nd ICMM, Rochester (NY), pp. 213–220.

Toh, K.C., Chen, X.Y., Chai, J.C., 2002. Numerical computation of fluid flow and heat transfer in microchannels. Int. J. Heat Mass Transfer 45, 5133–5141.

Tso, C.P., Mahulikar, S.P., 1998. The use of the Brinkman number for single phase forced convective heat transfer in microchannels. Int. J. Heat Mass Transfer 41, 1759–1769.

Tunc, G., Bayazitoglu, Y., 2001. Heat transfer in microtubes with viscous dissipation. Int. J. Heat Mass Transfer 44, 2395–2403.

Xu, B., Ooi, K.T., Mavriplis, C., Zaghloul, M.E., 2003. Evaluation of viscous dissipation in liquid flow in microchannels. J. Micromech. Microeng. 13, 53–57.

Zanchini, E., 1997. Effect of viscous dissipation on the asymptotic behaviour of laminar forced convection in circular tubes. Int. J. Heat Mass Transfer 40, 169–178.